

Experimental analysis of a compressed air engine with semi-gear mechanism

Mehdi Mostaghelchi¹, Javad Khadem^{2*}, Behzad Omidi Kashani³, Vali Kalantar⁴

¹Ph.D. Student in Mechanical Engineering, University of Birjand, Birjand, Iran

²Associate Professor, Faculty of Mechanical Engineering, University of Birjand, Birjand, Iran

³Assistant Professor, Faculty of Mechanical Engineering, University of Birjand, Birjand, Iran ⁴Associate Professor, Faculty of Mechanical Engineering, University of Yazd, Yazd, Iran

*Corresponding author: Javad Khadem

ABSTRACT

In this paper, a piston bidirectional compressed air engine with a semi-gear and rack mechanism in power transmission has been analyzed and investigated.

In this structure, there are two reciprocating pistons in two opposite positions to produce power. Therefore, there are two power courses in each rotation of the output shaft. In the power transmission mechanism, a rack gear and a semi gear have been used, so that the generating power is transferred to the rack gear through the reciprocating pistons and consequently to the semi gear and the output shaft.

The new engine first designed and after confirming the stress analysis of the parts in the software, it was made and then launched using compressed air energy. The data of this engine has been collected and analyzed using sensors and electronic equipment. The results of this research include experimental analysis, thermodynamic analysis and simulation of this new engine.

In the experimental results obtained from the performance of the mechanism in the form of a power generation engine, the average output speed of the engine at a relative pressure of 4.2 bar is 135 rpm, the engine output is equal to 495 watts.

The results of engine analysis through the extracted relationships, modeling solution, Simulation in Software and experimental data also indicate the overlap and appropriate consistency of engine analysis.

Key words: Compressed air engine, rack mechanism, semi-gear mechanism, piston bidirectional engine.

INTRODUCTION

1.Introduction and background

Today, increasing efficiency and reducing energy loss is very important and necessary, and extensive research has been conducted on optimizing and increasing the efficiency of energy-related mechanisms [1-5]. In their research so far, researchers have experimentally, numerically examined and simulated existing mechanisms, including cylinder-piston or rotary mechanisms and, each has tried to improve the performance of engines by presenting a new solution [6-11]. However, it is necessary to conduct extensive research on the investigation, presentation and analysis of new mechanisms in order to provide the most appropriate structure according to the application. Also, considering the limitations of using fossil fuels and reducing hydrocarbon fuel resources, attention to reducing pollutants in combustion engines, using available, renewable and environmentally friendly energy and using new structures such as compressed air mechanisms seem necessary [12-17].

Tamam Basbus et al. in 2012 [18], investigated the performance of a diesel engine as a four-stroke, two-stroke air-compressed, six-stroke, and the performance of a diesel engine as a compressor. The results of this study indicate the saving of engine fuel consumption, increased efficiency and very low emissions of carbon dioxide at a rate of 51 grams per hundred kilometers. In 2012, Guazi et al. [19] simulated the performance of an air engine in software. This research has proposed a mathematical model for a three-cylinder engine and, the dynamic characteristics of piston motion and gas parameters have been simulated and numerically solved. In 2013, Yung Huang et al. [20] used a cylinder engine and a crankshaft piston in the pressure range of 5-9 bar of compressed air to generate power. The results of this study indicate that the maximum power at 9 bar pressure at 1320 rpm is 0.95 kW.

Kanharaj et al. in 2014, [21] studied the thermodynamic analysis of a heat engine and a heat pump using the conditions of air phase change as a gaseous fluid in two phases, gas and liquid. Their results showed that by using a heat pump in the process of converting compressed air to liquid air, the efficiency is 70% and the efficiency in the reverse process is 53%. In 2014, Pathak et al. [22] presented an example of a compressed air vehicle of the rotary mechanism type, examining the engine output in different positions and declared the mechanical efficiency of compressed air engines in the pressure range of 4.1 to 7 bar at 3000 rpm equal to 55%.

In 2015, Dimitrova et al. [23] investigated the combined effect of using compressed air with a 3-cylinder internal combustion engine to generate power. The results of this study indicate a reduction in fuel consumption of the internal combustion engine, an improvement in efficiency by 50% and a reduction in carbon dioxide emissions. In 2015, Yu et al. [24] have evaluated a

compressed air engine equipped with a crankshaft. Results for the pressure of 20 bar, the maximum output power of 1.92 kW, the maximum output torque of 56.55 Nm and engine efficiency of 25% have been reported.

In 2015, Chi Liu et al. [25] used a compressed air single-cylinder engine to modify the inlet and outlet feed systems with different opening statuses of an engine. The engine used was able to provide 2.15 kW output power at the pressure of 13 bar with a torque of 15.97 Nm. In 2017, Marwania et al. [26] examined the technologies of power generation from compressed air and after various discussions have concluded that the use of compressed air in vehicles will be appropriate in the case of hybrid application. In 2016, Chi Min Liu et al. [27] have studied the expansion process in a two-stage air engine. The results of this study indicate an increase of about 12% in engine output power.

In 2017, Chi Min Liu et al. [28] transformed a four-stroke engine into a compressor to regenerate braking power in a variety of situations. The results showed that the maximum reduction pressure is 2.91 bar. In 2018, Fang et al. [29] developed an experimental sample to study energy recovery and power generation with compressed air technology. In this study, a diesel engine has been used and hot water was used as a heat source. The results show that under the influence of heat source, the maximum output power is 22% more than the output without heat supply. In 2018, Bravo et al. [30] analyzed brake recycling for heavy vehicles. The results show that the proposed system is able to store 69% of the available energy during a complete stop and 14% on a low slope on the highway.

As observed from the results, the method of implementation and analysis in the above research, each of them has examined the existing mechanisms and each of them have tried to improve the performance of engines by presenting a new solution. In the present paper, the performance of this structure in the form of a compressed air engine is evaluated, by presenting a new semi-gear and rack mechanism in power transmission.

2. New Engine Structure

According to Fig. 1, in the form of mechanism operation in the structure of a power generating engine, the three-way flow control valves in this situation connected the routes (1 to 2), (4 to 5), (7 to 8) and (10 to 11) to each other and the operating fluid will be able to pass through these paths. For example, if the main piston is at the far right, the mechanical fluid control rotary valve installed on Lines 8 and 2 is active. Compressed air now flows from the c-compressed air tank through the mechanical rotary valve installed in path 8 into the cylinder a, causing the piston to move to the left. In the left movement course of the piston, the air in the left cylinder chamber b is discharged into the environment by passing through a mechanical rotary valve installed in path No. 2. This condition will continue for up to a percentage of the piston stroke, after which the mechanical valve in Route 8 will close, but the valve in Route 2 will remain open. Now the flow of inlet fluid into the cylinder chamber a is stopped, but due to the pressure difference between the cylinder and the environment and due to the opening of the valve of route No. 2, the movement cycle of the piston will continue until the piston reaches the extreme left. In this situation, the rotary valve installed in route No. 2 is deactivated and the mechanical rotary valves in routes 5 and 11 are activated. In this case, the piston will move to the right due to the entry of fluid into the cylinder chamber from the left side of b and the discharge of air from the other side into the environment will move to the right. This situation will also be permanent up to a percentage of the piston course, then the rotary valve in path 5 becomes inactive and the mechanical valve in path 11 remains active. In this case, considering the pressure difference between the left chamber of the cylinder and the environment, the piston continues to move to the right to reach the end of its course. Now the valve of route 11 is deactivated and the valves installed in routes 8 and 2 become active and the course is repeated.

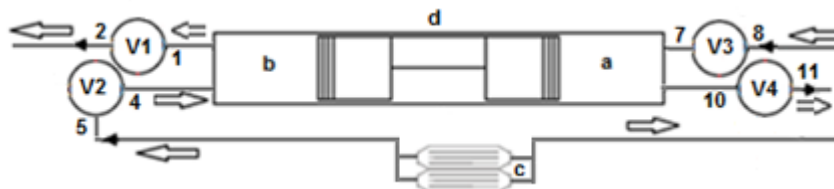


Fig. 1 Schematic of the engine

The semi-gear and rack gear mechanism has been also used to transmit power, as shown in Fig. 2. In this structure, the outlet shaft is connected to the pinion gear shaft and, the main cylinder piston to the rack gear. In this mechanism, in the power course of one of the pistons, the pinion gear engages the upper rack gear, and the linear motion of the piston and the rack gear leads to the rotational motion of the pinion gear. As the piston reaches the end of the power course, the pinion gear is simultaneously detached from the upper rack gear and engages with the lower rack gear. In this position, the other piston is at the beginning of the power course and the gas pressure leads to the linear movement of the piston and the rack gear, and consequently the pinion gear continues to rotate in the same rotational direction.

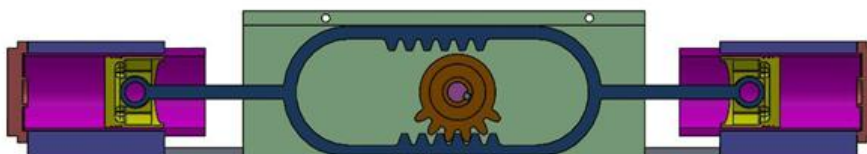


Fig. 2 Power transfer mechanism

In this engine, there are two power courses in each rotation of the output shaft, in other words, this single-unit engine is equivalent to a reciprocating 2 cylinder engine. It is also possible to change the velocity and torque of the output shaft with constant engine power. Since in the structure of semi-gear and rack gear, the output torque of the engine is equal to the output force of the power-generating pistons at the average radius of the semi-gear. Therefore, as the radius of the semi-gear is increased, the torque applied to the output increases. The linear velocity of the piston is equal to the product of the angular velocity of the output shaft in the average radius of the semi-gear, and the output angular velocity rate is reduced with increasing the radius of the semi-gear. Therefore, in the output power status of the engine cylinders, the torque increases and the angular velocity decreases with increasing semi-gear diameter.

2-1. Description of the fabricated engine parts

This type of engine consists of a bidirectional piston cylinder chamber with a piston diameter of 71 mm and a course of 134 mm in each cylinder, two-cylinder heads, mechanical rotary valves for fluid flow control, a power transmission mechanism, outlet steel shaft, two flywheel, compressed air storage tank and fluid transfer tubes have been formed as shown in Fig. 3.

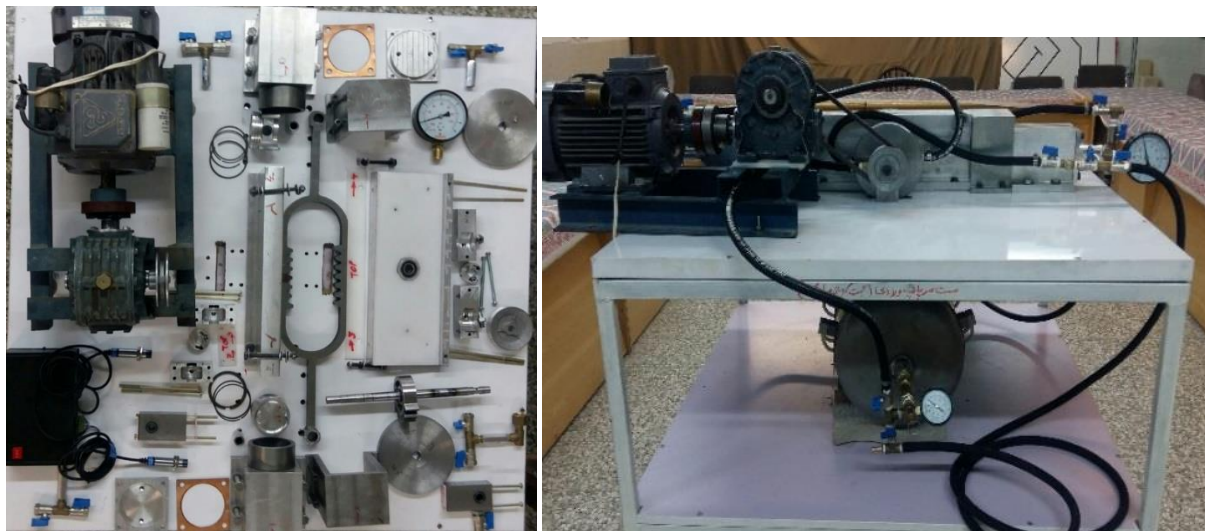


Fig. 3 Engine in two modes of assembly and disassembly

The pistons have reciprocating linear motion inside the cylinder housing, and this motion is transformed into rotational motion through the power transfer mechanism. The double rack gear has two connection points to the pistons, which are connected to the pistons by connecting the pin. The semi-gear is engaged with the upper rack gear in the zero to 180 degree angular phase where one piston is in the expansion course and the other piston is in the discharge course. It is connected to the lower rack gear at an angle of 180 to 360 degrees, the various situations of which have been shown in Fig. 4.

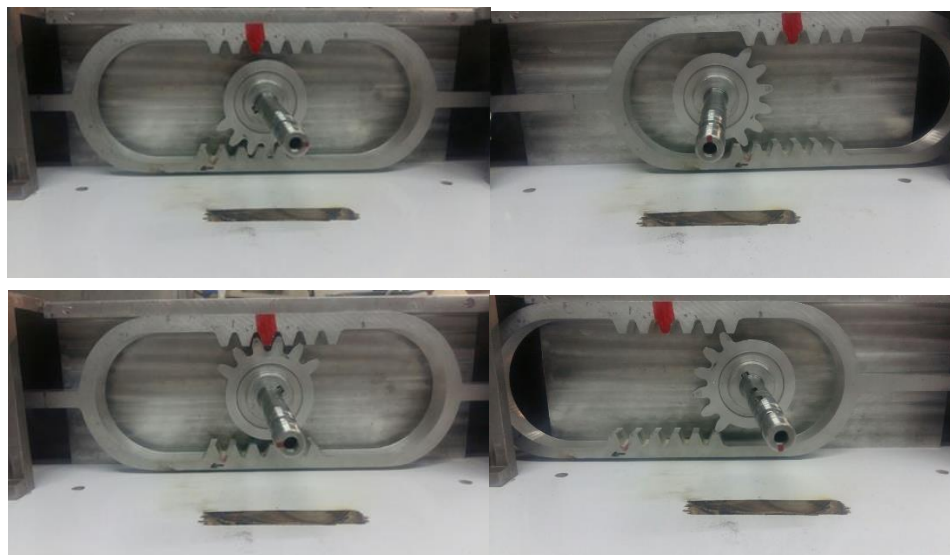


Fig. 4 Semi gear and rack engagement situations

Mechanical rotary valves are designed in such a way that a valve has been considered to control the entry of compressed air from the tank and a valve to control the discharge of air from the engine chamber, for both sides of the cylinder. High-pressure air is established from the storage tank to the area behind the mechanical rotary valves, and as the inlet path is opened by rotating the valve, the compressed airflow to the cylinder chamber generates power and causes the piston to move. Air is discharged from the cylinder chamber into the environment through another mechanical rotary valve and by opening the exhaust duct which receives its command from the outlet circulation. Rotary valves, one for inlet flow control and the other for outlet flow control, have been

shown in Fig. 5. The control valves and holder blocks are located on either side of the holder chambers of the semi-gear and rack gears, and the engine output shaft passes through the middle of the control valves. The rotary valves are fixed on the engine output shaft and rotate with the outlet shaft. The inlet valve holder block has a compressed air inlet duct from the tank and has two outlet ducts to feed the cylinders, and the position of the rotating valve will determine which cylinder the compressed air will flow to. The outlet valve holder block also has two inlet ducts from the cylinders and a discharge duct into the environment.

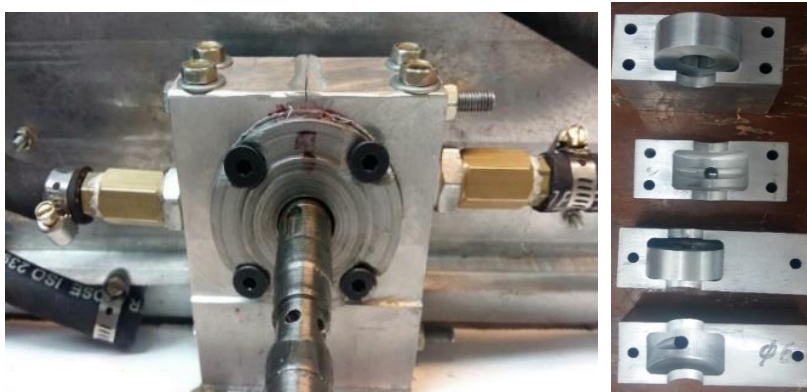


Fig. 5 Rotary valves for fluid flow control

3. Equations and Related Relationships

3-1. Analysis of thermodynamic theory diagram and rotary inlet and outlet valves of fluid flow control

According to the results of research conducted in references [23] and [29] to [31] and [34-35], the closest thermodynamic cycle in each 180 degree course consists of two iso bar processes, two iso volume processes and one isentropic process according to Fig. 6. Since the high-pressure gas inside the tank is supplied and located in the area behind the inlet valve, by opening the inlet valve at point 5, high-pressure gas enters the cylinder chamber and the constant pressure inside the cylinder chamber reaches the maximum pressure at point 1. In processes 1-2, the inlet valve is open, which leads to the movement of the piston, the expansion process can be considered as a constant pressure process. At point 2, the inlet valve is closed and the expansion process is complete. At point 3, the outlet valve is opened and the pressure inside the cylinder decreases to the ambient pressure. Process 4-5 is mechanical evacuation. When the piston reaches point 5, the outlet valve is closed and the inlet valve is opened and the pressure inside the cylinder will reach maximum pressure.

According to the PV diagram of the engine, the known parameters are:

Pressures P_2 and P_1 are assumed to be equal to 500 kPa, pressure P_3 is assumed at 200 kPa and pressure P_4 is assumed to be 100 kPa. The dead volume (V_1) of the cylinder is 60 cm^3 , the volume of the cylinder at the end of the lower dead point is 595 cm^3 . The unknown parameters V_2 and T_2 are obtained by using adiabatic expansion relationships equal to 309 cm^3 and 110 degrees Celsius, respectively. According to the known position of point 2, the distance at which the inlet valve of the cylinder is open will be equal to 88 mm of the piston course and approximately 90 degrees of rotation of the outlet shaft.

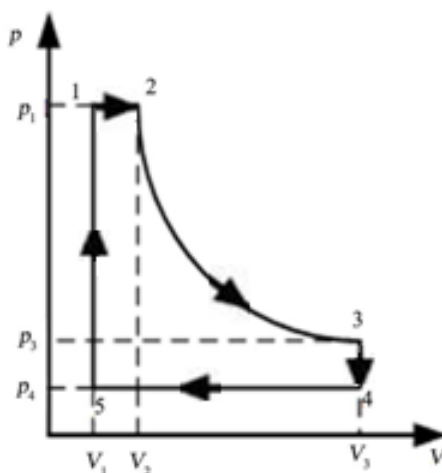


Fig. 6 Thermodynamic P-V diagram of the engine

In the structure of the available engine, the diameter of the mechanical rotary valves for dividing the flow of the operating fluid is equal to 40 mm, so the value of the valve perimeter will be equal to 126 mm. On the other hand, the diameter of the hole embedded in the mechanical rotary valve is equal to 8 mm and has a cross-sectional area of 50 mm. Now, if 126 mm of valve perimeter is equal to 360 degrees, the 8 mm hole of the fluid will be equal to 23 degrees. Since, according to the theoretical thermodynamic PV diagram, it is necessary to open the inlet valve at an angle of 90 degrees from the output shaft and then close it, it is also necessary to keep the mechanical rotary outlet valve open during the discharge process at the 180-degree phase of the shaft. According to the

predicted structure at the 360-degree phase of the engine output shaft rotation, the inlet rotary valve starts to open from a zero-degree angle of the rotating shaft where the piston of one of the cylinders is at the high dead point and, this increase in the cross-section of the inlet will continue until the angle of 23, because the inlet valve needs to be left 90 degrees open from the point onwards, until the angle of 113 degrees (90 + 23) is completely open and from the angle of 113 degrees it starts to close and, it closes completely at an angle of 136 degrees (23 + 113). At the end of the expansion process, the other cylinder piston reaches a high point of death, and since the geometric parameters of both cylinders are the same, then, the inlet valve of the new cylinder starts to open at the angle of 180 degrees, completely opens at an angle of 203 degrees and, is in the fully open phase at an angle of 203 to 293 degrees. The inlet valve begins to close at an angle of 289 degrees, and it closes completely at an angle of 316 degrees. There is also a special timing in the mechanical rotary outlet valve so that the outlet rotary valve from the zero degrees angle of the rotating shaft where the opposite cylinder piston, which is located at the lower point of death, begins to open, and opens fully to the angle of 23 degrees, fully opens at the angle of 23 degrees to 157 degrees and closes completely at the angle of 180 degrees. Then, the discharge phase of another cylinder has started therefore, the outlet rotary valve starts to open the exhaust cylinder of the other cylinder from an angle of 180 degrees and opens completely at an angle of 203 degrees. From this angle, the outlet valve is completely open up to 327 degrees by the outlet rotary valve and then it gradually starts to close and closes completely at a 360 degree angle. This cycle of inlet and outlet rotary valves is constantly repeated.

The operating diagram of each of the mechanical inlet and outlet rotary valves is as shown in Fig. 7 below:

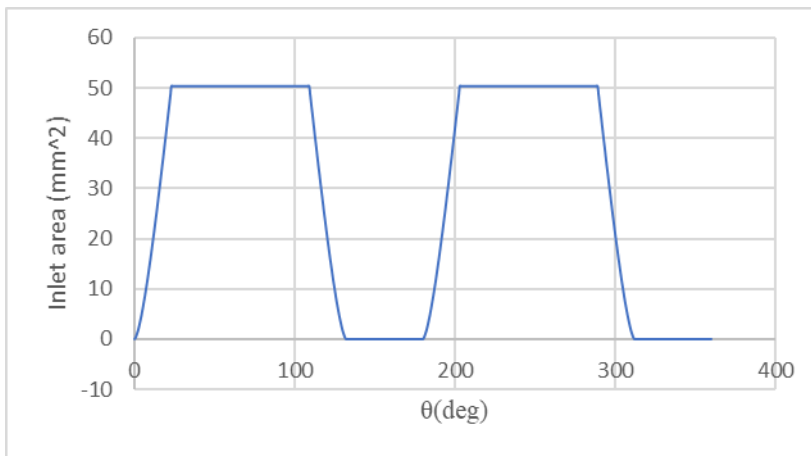


Fig. 7-a Inlet valve diagram

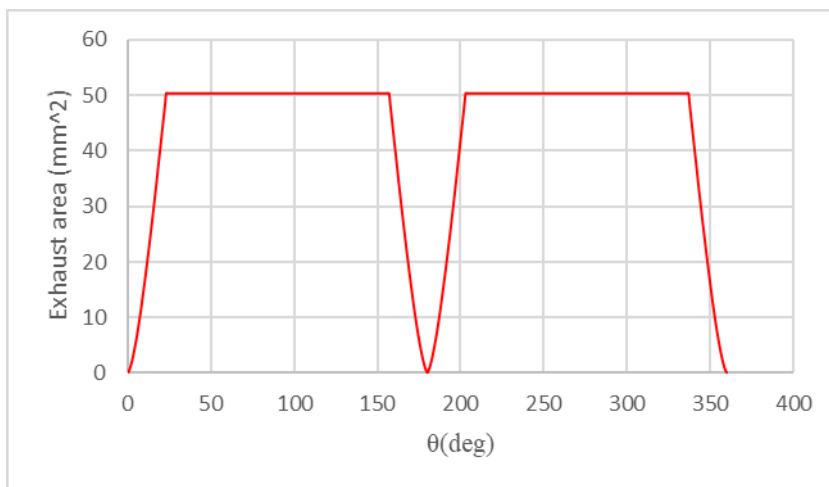


Fig. 7-b Outlet valve diagram

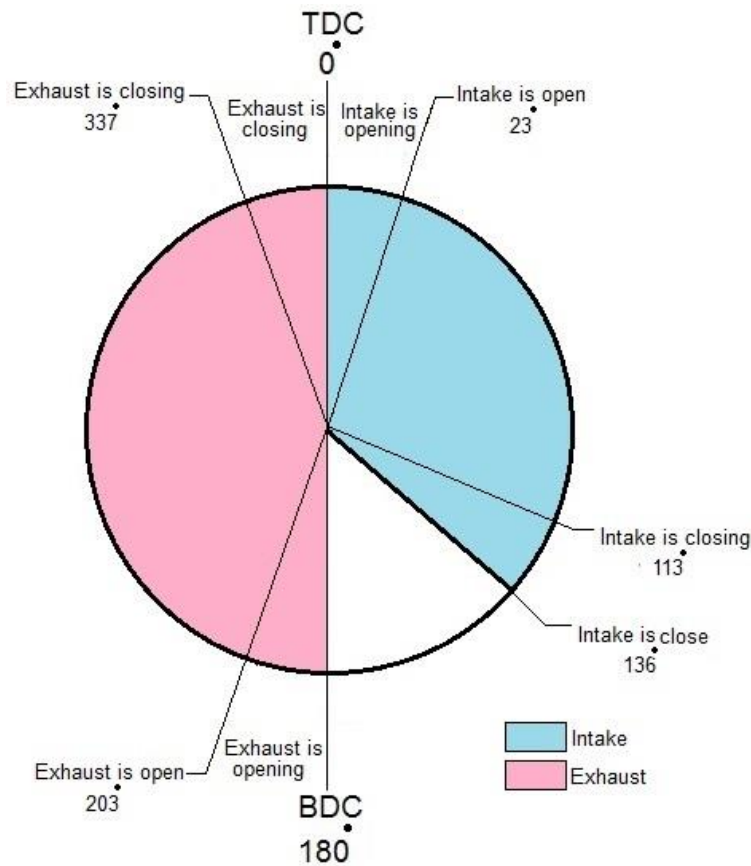


Fig. 7-c Inlet and outlet valve function

3-2. Calculation of the theoretical power generation

A: Calculation of the work generated when the inlet valve is open (Process 1-2).

$$W_{1-2} = P_1(V_2 - V_1) \quad (1)$$

Where P_1 is inlet pressure, V_2 is the volume of the piston when the inlet valve is closed, V_1 is the volume of the piston when the inlet valve is open and the cylinder chamber begins to expand.

B: Calculation of the work generated when the inlet valve is closed (Process 2-3).

Given that process 2-3 is an isentropic process, and since k is defined as the specific heat ratio, the generated work in this process will be as follows:

$$W_{2-3} = \frac{P_3V_3 - P_2V_2}{1 - k} \quad (2)$$

C- Calculation of the work consumed in process 4-5:

The work consumed in this process is provided by the work generated by another expanding piston. The amount of this work is equal to:

$$W_{4-5} = P_4(V_1 - V_3) \quad (3)$$

According to parts A to C, the net work produced by each cylinder in one cycle is estimated as follows:

$$W_{net} = P_1(V_2 - V_1) + \frac{P_3V_3 - P_2V_2}{1 - k} + P_4(V_1 - V_3) \quad (4)$$

If the proposed engine speed is equal to n rpm, the output power by the two cylinders can be calculated from the following equation (5):

$$P_w = 2 \times W_{net} \times \frac{n}{60} \quad (5)$$

3-3. Speed and related parameters according to the output shaft angle

To determine the piston speed at any given moment, we must calculate its kinetic energy at any given moment. To do this, we must first calculate the energy injected into the set by the gas inside the piston.

According to the law of conservation of energy, if we denote the initial volume of the cylinder by V_1 and the volume of the cylinder at any given moment by V , the work produced by the gas inside the cylinder at any given moment is equal to $W = \int_{V_1}^V P dV$, where p is the instantaneous pressure inside the cylinder. Some of this energy is used to overcome the friction between the piston and the cylinder wall $\int_0^\theta 2\mu N r d\theta$, some of it is used to move the pistons, shaft and flywheel [32] $\int_0^v \left(m + \frac{I_0}{r^2}\right) v dv$, The rest is as pure work or renitent torque applied to the output shaft $\int_0^\theta T d\theta$. μ is the coefficient of friction between the piston and the cylinder wall, N is the vertical force on the cylinder wall, r is the semi-gear radius which is approximately equal to the mean inner and outer semi-gear radius, θ is the angle of the output shaft (radians) and I_0 is the sum of inertia, semi-gear and the flywheel around the output shaft.

So there is:

$$\int_{V_1}^v P dV = \int_0^v \left(m + \frac{I_0}{r^2}\right) v dv + \int_0^\theta 2\mu N r d\theta + \int_0^\theta T d\theta \quad (6)$$

By integrating from the above equation (6), the piston speed can be calculated:

$$v = \sqrt{\frac{2W - 4\mu N r \theta - 2 \int_0^\theta T d\theta}{m + \frac{I_0}{r^2}}} \quad (7)$$

Since the velocity of the piston is equal to the product of the radius of the semi-gear and its angular velocity; the angular velocity of the semi-gear and all rotating parts can be calculated as follows (8):

$$\omega = \frac{1}{r} \sqrt{\frac{2W - 4\mu N r \theta - 2 \int_0^\theta T d\theta}{m + \frac{I_0}{r^2}}} \quad (8)$$

ω is the angular velocity of the output shaft, T is the output torque of the engine and m is the sum of the mass of the two pistons and the two rack gears, and in general each part with reciprocating motion with the piston. To obtain the acceleration of the piston, it is sufficient to calculate the result of the forces acting on it and divide it by the mass of the piston.

$$a = \frac{\left((P - P_4)A - 2\mu N - \frac{T}{r} - \left(\frac{I_0 \omega^2}{2r}\right)\right)}{m} \quad (9)$$

The result of the forces acting on the piston are: The force due to the gas pressure inside the cylinder, which is equal to $(P - P_4)A$ at any moment. this force is the driving force and increases the acceleration of the piston. The friction force between the piston and the cylinder wall is equal to μN . Since both pistons are moving at any given moment; the friction force of both pistons is $2\mu N$. This force is a resistive force and reduces the piston acceleration. the value of μN has been measured experimentally and has been estimated at 100 N. The force applied from the semi-gear to the rack gear, which is a resistive force and reduces the acceleration of the piston. The reaction of this force, i.e. the force applied by the rack gear to the semi gear, leads to the rotation of the rotating parts and creates the output torque of the engine. The acceleration of the piston is obtained by dividing the result of the mentioned forces by the mass of the piston (mass of all the parts connected to the piston).

The rack gear is in direct contact with the semi gear and the linear displacement of the rack gear (equivalent to the displacement of the piston) is equal to the length of the arc associated with the rotation of the junction of the semi gear with the rack gear.

$$x = r\theta \quad (10)$$

x defines the instantaneous position of the piston and $x=0$ refers to the position of the piston when the cylinder has the smallest volume. According to the structure of the mechanism, $x=0.134$ is related to the position of the piston when the cylinder has the maximum volume.

r denotes the radius of the semi-gear, which has been considered to be equal to 43 mm therefore, the engine rotation angle is equal to 180 degrees per piston course.

Since $dV = A dx$ and $dx = r d\theta$, the equation for the piston speed in terms of the output angle of the shaft is as follows (11):

$$v = \sqrt{\frac{2 \int_0^\theta P A r d\theta - 4 \int_0^\theta \mu N r d\theta - 2 \int_0^\theta T d\theta}{m + \frac{I_0}{r^2}}} \quad (11)$$

The piston speed at each stage of cylinder expansion is also obtained as follows:

A: When the piston is expanding and the inlet valve path is open to either side of the piston:

$$v = \sqrt{\frac{2(P_1(V_2' - V_1) - P_4(V_2' - V_1)) - 4\mu N r \theta - 2 \int_0^\theta T d\theta}{m + \frac{I_0}{r^2}}} \quad (12)$$

B: When the piston is expanding and the inlet valves are closed (assuming the expansion process in the isentropic state):

$$v = \sqrt{\frac{2 \left(P_1(V_2 - V_1) + \frac{(P_3' V_3' - P_1 V_2)}{1 - k} - P_4(V_3' - V_2) \right) - 4\mu N r \theta - 2 \int_0^\theta T d\theta}{m + \frac{I_0}{r^2}}} \quad (13)$$

Where, V_2' denotes the cylinder volume at each outlet shaft angle in the constant pressure expansion process, V_3' represents the cylinder volume at each outlet shaft angle in the isentropic expansion process, P_3' is the cylinder pressure at each outlet shaft angle output process in the isentropic expansion process.

3-4. Investigation of the force applied to the mechanism and stress analysis in all parts

The semi gear and the rack gear are connected and apply force at the joint (Fig. 8). The work produced by this force is equal to the amount of this force multiplied by the displacement of the point of effect of the force. Therefore the differential value of this work is equal to: $Frd\theta$

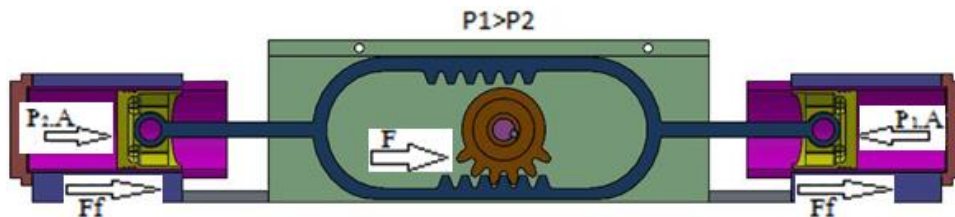


Fig. 8 Diagram of forces

A part of this work is used to move the rotating parts and the rest is considered as output work. The differential form of the energy required to move the rotating parts is equal to $I_0 \omega d\omega$ and the differential form of the energy generated by the engine output torque is $Td\theta$. So we have:

$$Frd\theta = I_0 \omega d\omega + Td\theta \quad (14)$$

By integrating from equation (15), the amount of force applied to the semi gear as well as the rack gear, at any given moment, is equal to:

$$\int_0^\theta Frd\theta = \frac{1}{2} I_0 \omega^2 + \int_0^\theta Td\theta \quad (15)$$

The average horizontal force on the rack gear for the output shaft angle of between 0 and θ is as follows:

$$\bar{F} = \frac{\frac{1}{2} I_0 \omega^2 + \int_0^\theta Td\theta}{r\theta} \quad (16)$$

It should be noted that all the components in the mechanism have been analyzed under stress in software and the results of the analysis showed that the maximum applied stress was in the rack gear area and, according to the materials used and the dimensions of the parts in the design the stress is 275.14 MPa, which is much less than the yield stress of steel, which was equal to 380 MPa, which has been shown in Fig. 9.

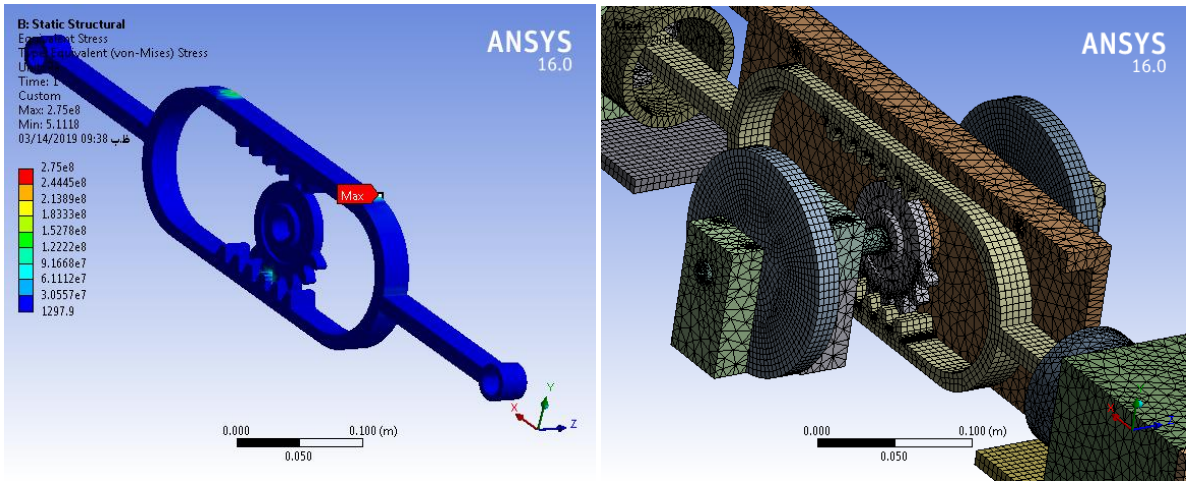


Fig. 9 Investigation of stress in rack gear

4. Theory Analysis

4-1. Engine performance analysis according to the extracted relationships

According to the basic known parameters and considering the expansion process in the adiabatic state and using the corresponding relationships, the unknown parameter V_2 will be equal to 0.000309 m^3 .

In reference [24], there is also a relationship to determine the engine efficiency:

$$\eta = \frac{P_1(V_2 - V_1) + \frac{1}{1-k} P_1 V_2 \left[\left(\frac{V_3}{V_2} \right)^{1-k} - 1 \right] + P_4(V_2 - V_3)}{P_1 V_2 \ln \frac{P_1}{P_4}} \quad (17)$$

which has been used to determine the position of point No. 2 of the theoretical diagram that provides the maximum possible efficiency according to the known thermodynamic properties. So that if $\frac{\partial \eta}{\partial V_2} = 0$, the appropriate volume of the cylinder chamber in which it is necessary to close the compressed air inlet into the cylinder will be equal to $V_2 = 0.00024 \text{ m}^3$. The comparison of this volume with the volume obtained from the relationships related to adiabatic expansion overlapped with each other and indicates that the position in which the inlet valve has been considered to close is a good position.

According to the specified parameters, the piston speed variation diagram is extracted from Equations (13) and (16) as shown in Fig. 10. Also, the changes of pressure inside the cylinder with respect to the position of the piston, are obtained from the relationship of the adiabatic expansion process according to the angle of the outlet shaft, which has been shown in Fig. 11.

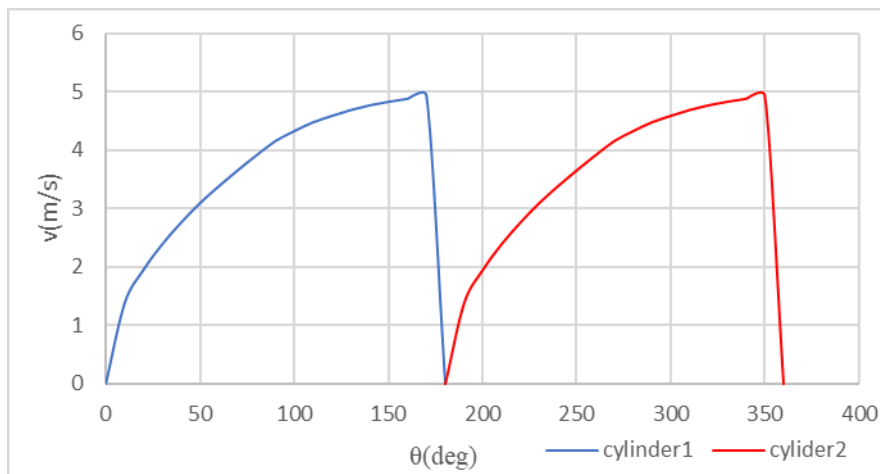


Fig. 10 Diagram of velocity variation in terms of shaft angle

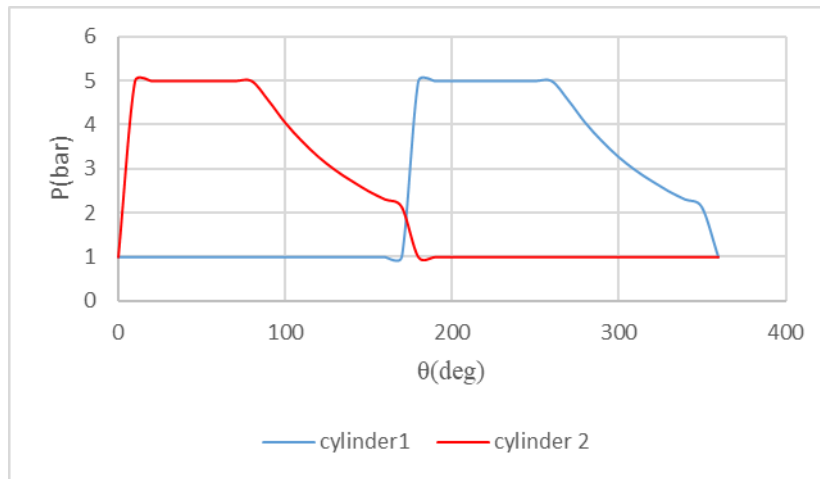


Fig. 11 Diagram of pressure variation in terms of angle

The average velocity of the piston and consequently the average velocity of the engine will be equal to 700 rpm with the average velocities and rounds obtained from the velocity-related equations. Also, due to the known volume difference between points 1 and 2 of the PV theory diagram, and the resulting engine velocity, the flow rate will be equal to 350 liters per minute and the output power will be about 3750 watts.

4-2. Engine Performance Analysis from Air Engine Modeling

In order to simulate the engine mechanism with semi-gear and rack structure to analyze the dynamic characteristics of piston motion and operating fluid parameters, some results and analyzes performed in references [19] and [33] have been used to be able to analyses and achieve the result benefited from the performance and status of the effective parameters in the performance of the engine mechanism.

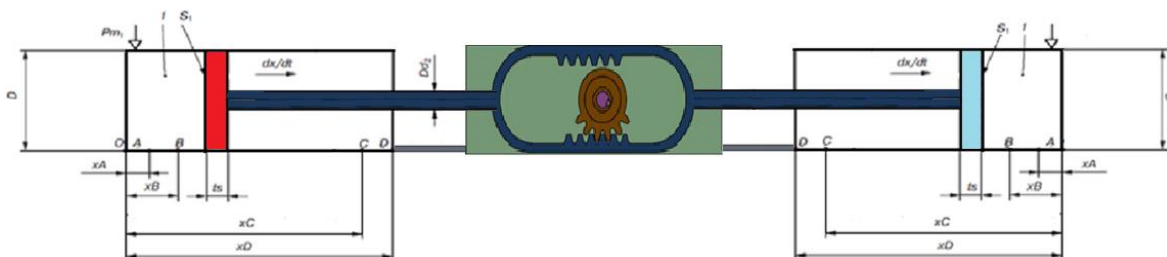


Fig. 12 Schematic of the cylinder and piston

According to Fig. 12, the piston is initially in position A. The value of x_A is the distance between the end of the cylinder and point A, which is determined by the user as the program input. The values x_B , x_C and x_D are also introduced to the program according to the geometry of the cylinder and piston. The simulation process starts from point A and continues until the piston reaches point D. The values of pressure inside the cylinder when the piston is between position x_A and x_C are calculated by the following equation:

$$\frac{dP_1}{dt} = \frac{K\mu_1\alpha_1 k P_1 \Phi(\sigma) \sqrt{R \cdot T_{m1}}}{V_1} - \frac{k P_1 dV_1}{V_1 dt} \quad (18)$$

Where, P_1 is the pressure inside the cylinder at any time, α_1 is the area of the air inlet duct and μ_1 is the flow coefficient. σ is defined as the ratio of the pressure inside the cylinder to the pressure inside the manifold. The function Φ is a function in terms of σ and is written as follows:

$$\Phi(\sigma) = \sqrt{\sigma^{\frac{2}{k}} - \sigma^{\frac{k+1}{k}}} \quad (19)$$

Where, k is the coefficient of specific heat ratio of the gas. The expression K is also defined in the equation (20) as follows:

$$K = \sqrt{\frac{2k}{k-1}} \quad (20)$$

V_1 is the volume of the cylinder at any time and is determined according to equation (21):

$$V_1(t) = A_p \times x(t) = A_p \times r \times \theta \quad (21)$$

Where, A_p is the area of the piston and $x(t)$ is the position of the piston at any given moment. As the piston passes through the x_B position, the pressure change values are determined in terms of time from equation (22).

$$P_1 = P_{1B} \left(\frac{XB - ts}{X - ts} \right)^n \quad (22)$$

t_s denotes the piston thickness and power n is related to the pressure changes according to the piston position and are calculated as follows:

$$n = 1 + \frac{[\sigma_0 - 1]}{\sigma} \quad (23)$$

Where, σ_0 is the ratio of static pressure inside the cylinder to the manifold pressure and σ is the ratio of pressure inside the cylinder to the manifold pressure. The values of $x(t)$ are determined by Newton's second law.

$$\frac{d^2x}{dt^2} = \frac{P_1 A_p - P_2 A_p - F}{M} \quad (24)$$

Where, P_1 is the air pressure inside the cylinder which leads to the production of power, P_2 is the pressure of the cylinder on the opposite side which is in the discharge course, F is the resistance force between the cylinder and the piston and is due to the force of the rings and M is the mass of the piston. The mass of the rack gear and the mass equivalent to the rotating parts considered as equivalent mass.

The results of this analysis are in accordance with the following graphs (Figs. 13, 14, 15).

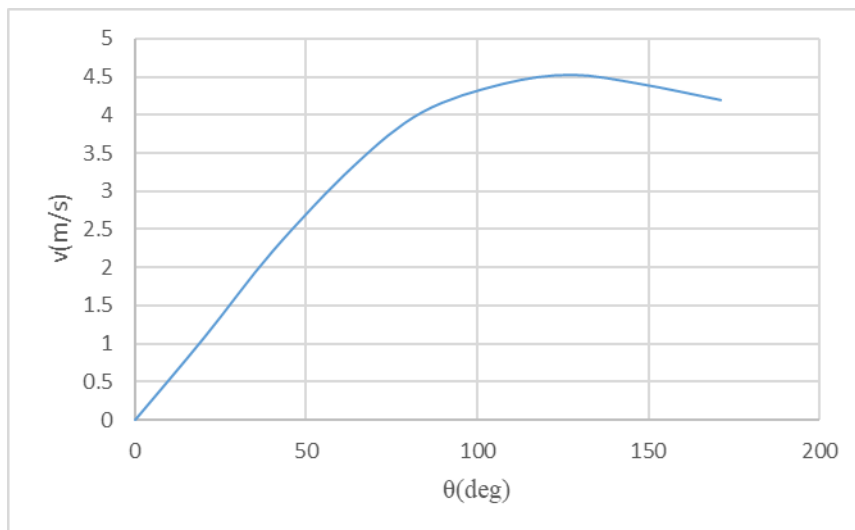


Fig. 13 Piston velocity variation in modeling

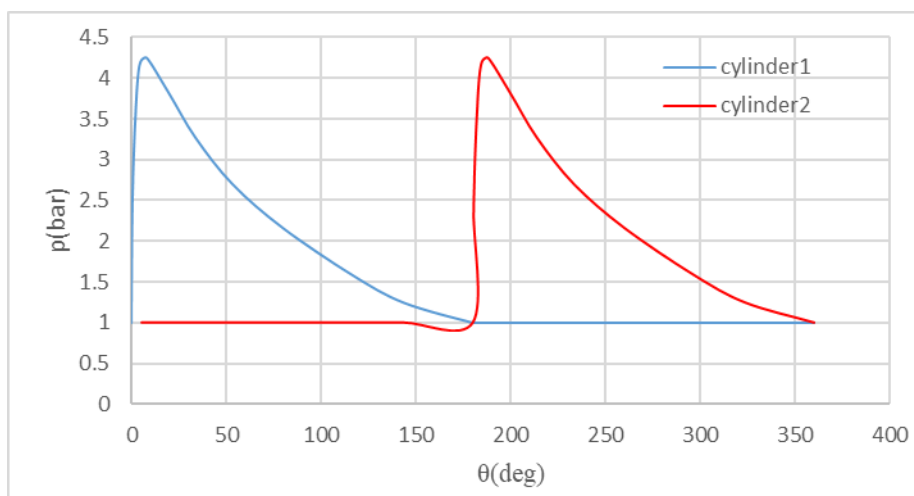


Fig. 14 Cylinder pressure variation in modeling

The power generated by the engine is equal to the product of the pressure inside the cylinder, the area of the piston and its velocity and since instantaneous velocity and pressure are available, the instantaneous power generated by the engine can be extracted as shown in Fig. 15.

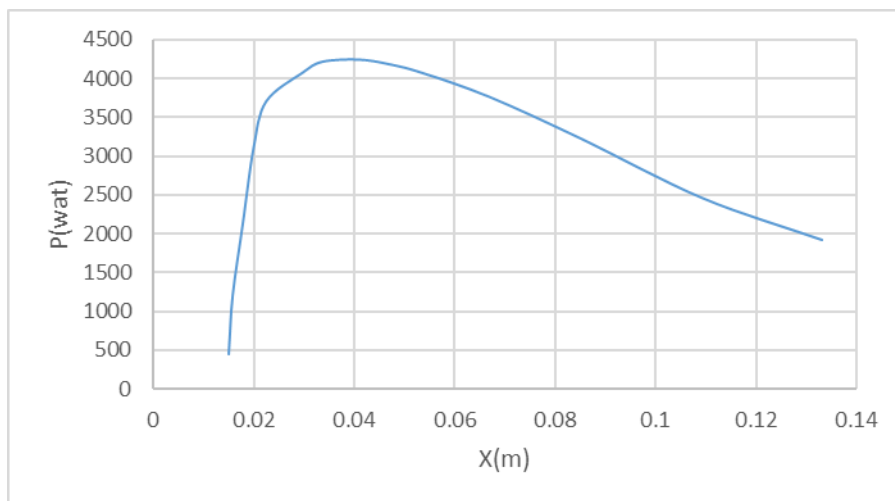


Fig. 15 Power generation in terms of displacement in modeling

According to the diagram of piston speed variation from engine modeling, the average engine round will be equal to 670 rpm. According to the area below the power-displacement curve, and the known average round, the output power of the engine is set at 4700 watts and, due to the fact that the inlet valve is an open course and consequently the volume of inlet air to the cylinder and the existence of a known average velocity, the flow rate will be equal to 360 liters per minute.

4-3. Schematic analysis of the engine

The schematic of the operation of the equipment used in the mechanism has been shown in the figure below (Fig. 16). In engine operation, valves 14, 18, 32 and 33 are closed and valves 13, 17, 29 and 30 are open. As valve 10 is opened to activate the structure, the fluid flow from the tank is directed to flowmeter 11 and the mechanical rotary valve of inlet 12 is directed as the inlet flow divider. The position of the mechanical rotary valve determines the airflow to one of the two valves No. 13 or 17, which will eventually lead to the movement of the actuator piston. The air on the other side of the cylinder chamber, due to the predetermined timing of the engine in the outlet mechanical rotary valve No. 31 as an outlet divider through one of the two valves No. 29 or 30 is discharged into the mechanical rotary valve and into the environment. As structure No. 16 is moved, the generated work is transferred to generator No. 28 through gearbox No. 26 so that it can be used to measure the generation power. The output shaft velocity can also be measured with an optical odometer No. 25. To determine the pressure-volume diagram and consequently measure the internal power of the engine, a pressure sensor of piezoelectric type 21, encoder No. 24, data logger No. 22 and processor No. 23 have been used and instantaneous changes in pressure inside the cylinder can also be seen through manometer No. 20. Valve No. 4 and compressor No. 1 can also be used for immediate discharge or possible charging of tanks.

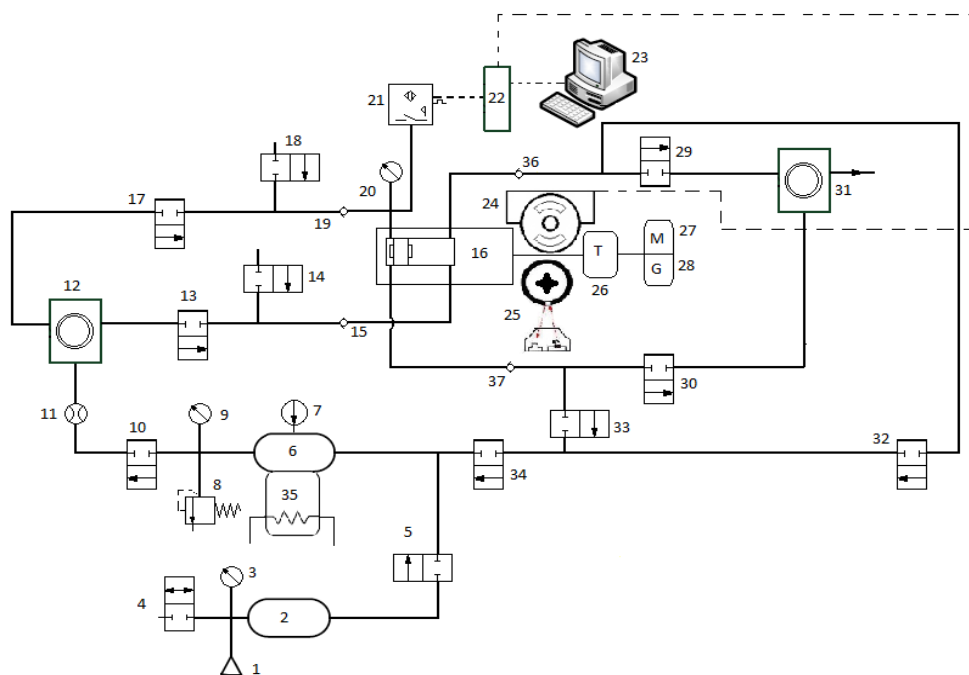


Fig. 16 Schematic of the engine with the components

5. Extraction of Results and Experimental Analysis

The minimum starting pressure of the mechanism in real conditions was observed at an absolute pressure of 1.8 bar and considering that in the calculations, the minimum pressure at the end of the piston course is considered at 2 bar therefore, this will confirm the assumptions of mathematical and thermodynamic calculations.

The required flow rate was calculated according to the extracted relations to produce the maximum power according to the known parameters of 350 liters per minute. But since this flow rate is less than this value and equal to 100 liters per minute for each of the engine cylinders according to the routes and materials used in real conditions. Therefore, achieving a lower velocity than the predicted velocity and also lower power than the desired limit has been possible. Fig. 17 shows the measurement of consumption flow rate and average engine velocity.



Fig. 17 Engine speed and flow rate measurement equipment

After starting the engine, measuring equipment has been used in order to provide the possibility of testing and creating conditions for data collection from the engine to achieve the result. In order to measure the internal work of the diagram obtained from the PV diagram in this structure, a pressure sensor from the German company Kistler and model 6613CA has been used on the cylinder head, a rotary encoder from Atonik Company of South Korea, model E50S8-3600-6- L-5 on the output shaft and a data logger to record data to measure and record instantaneous pressure values, also, a generator has been installed in the engine output to be able to measure the engine output power, which has been shown in Fig. 18. The internal work of the engine is equal to the enclosed surface of the PV diagram. The product of the work obtained from the pressure-volume diagram in the number of engine revolutions will indicate the internal power of a cylinder and since this engine is a two-cylinder engine the total power will be doubled, the difference between the measuring power produced by the generator and the internal power indicates the power loss.

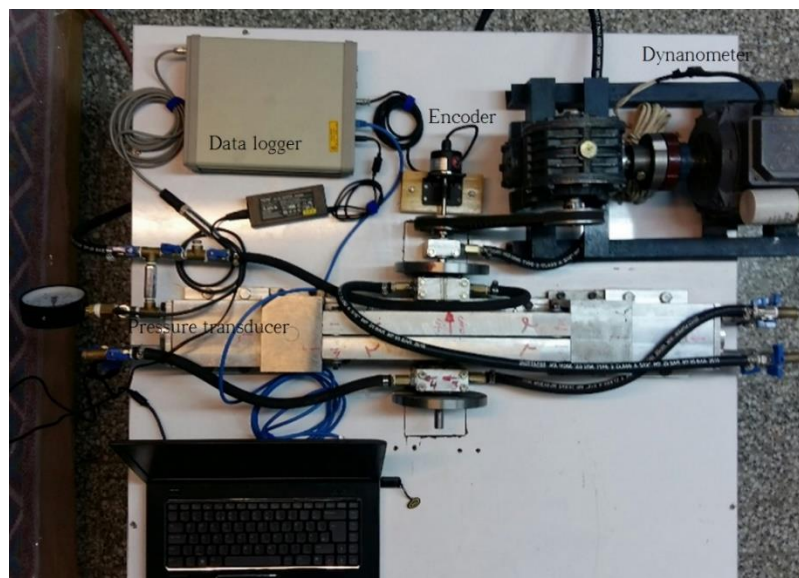


Fig. 18 Data measurement and recording equipment

In this situation, many experimental diagrams of pressure changes in terms of the output shaft angle at different pressures and cycles have been obtained according to the available parameters, which are shown in Fig. 19 related diagrams.

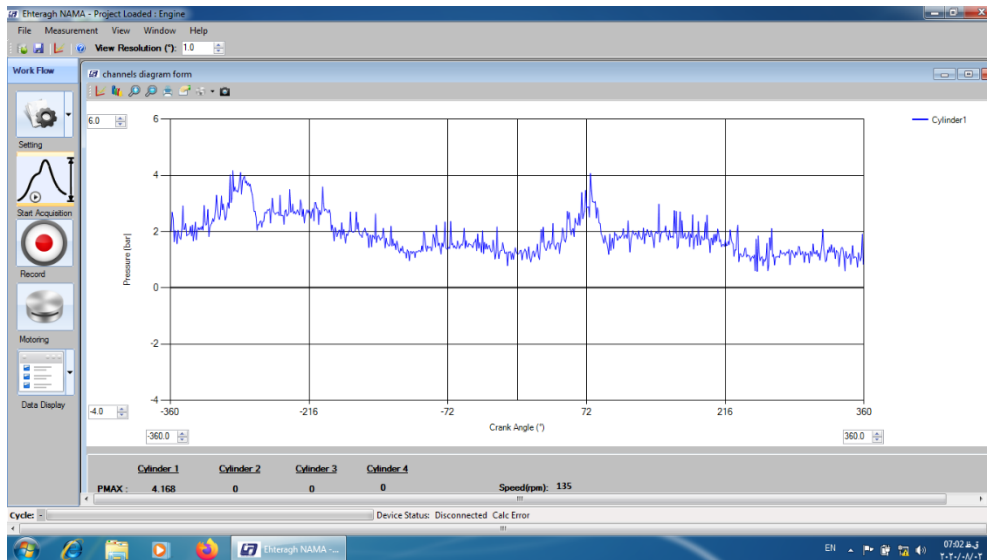


Fig. 19 An example of the recorded experimental diagram

According to the experimental diagrams extracted from the engine, by adapting a large number of graphs at the corresponding pressures and operating speeds and using software, after smoothing and normalization, the final diagrams have been extracted based on P θ and PV.

At a pressure of 4.2 bar in the cylinder, the engine speed has reached an average of 135 rpm. By calculating the enclosed surface of the curve, the amount of work obtained is equal to 221 joules per cycle of the output shaft for each cylinder. Therefore, the output power of the engine will be equal to 495 watts. Generation power is transmitted through the semi-gear and rack mechanism from the belt wheel mechanism installed on the engine output shaft to the gearbox. Finally, the output shaft of the gearbox will act as the driver of the generator and finally 237 watts of electrical power became available.

Diagrams of pressure in terms of the rotation angle of the output shaft and pressure in terms of volume have been shown in Fig. 20

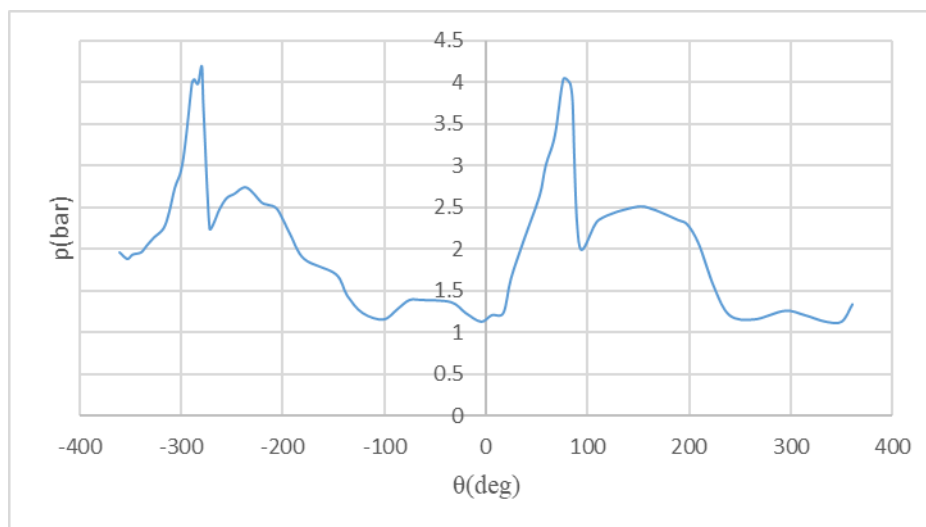


Fig. 20-a Experimental P θ diagram

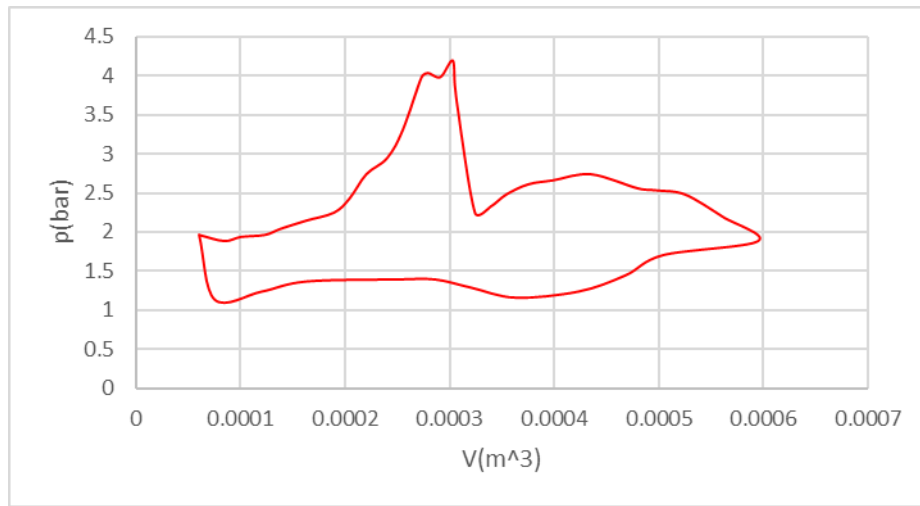


Fig. 20-b Experimental PV diagram

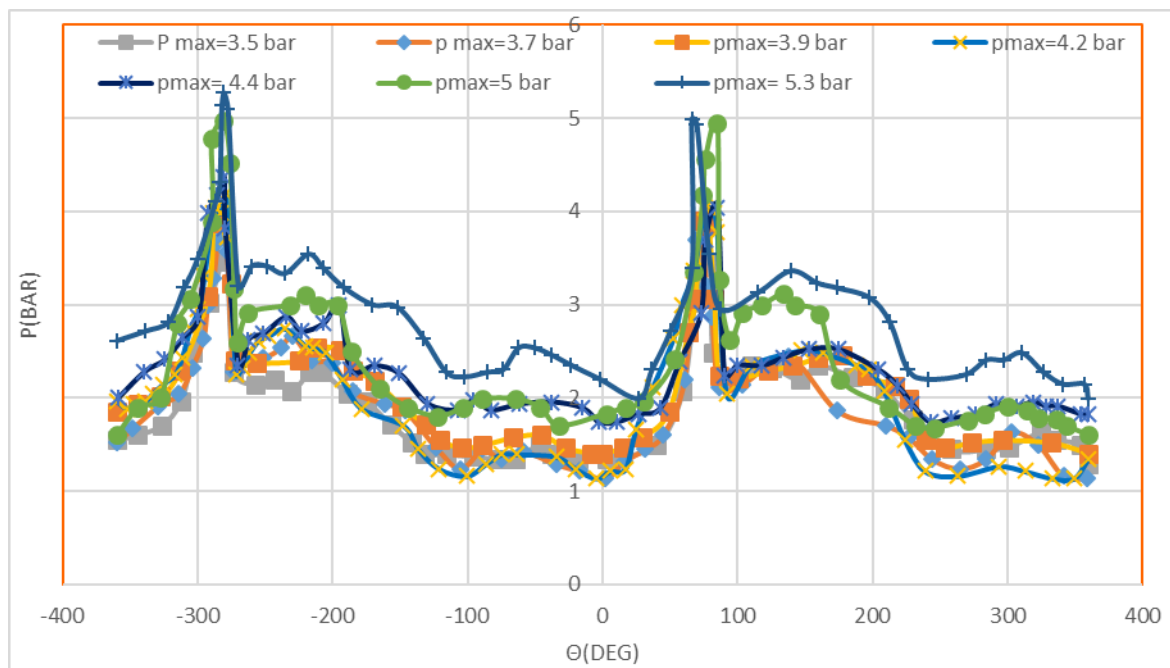


Fig. 20-c Experimental Pθ diagram at different pressures

6. Simulations in software

the issue is examined using software to be able to examine the engine in different analytical situations. For this purpose, the dynamic mesh method has been used to simulate the movement of the piston using Ansys Fluent software. for cylinder motion mesh, layering method and for rotary valve mesh, remeshing method has been used. in selecting the model, the Inviscid assumption is used, and the Coupled method is used in selecting the solution method, and Presto has been selected in order to solve the pressure equations. The results of simulation at software have been shown in Figs. 21.

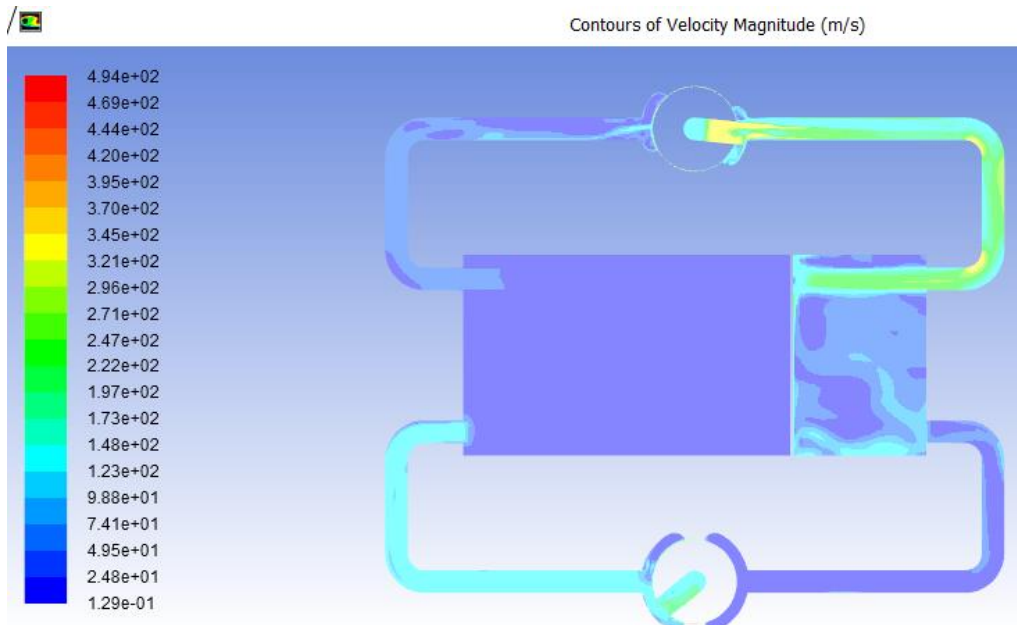


Fig. 21-a contours of velocity magnitude

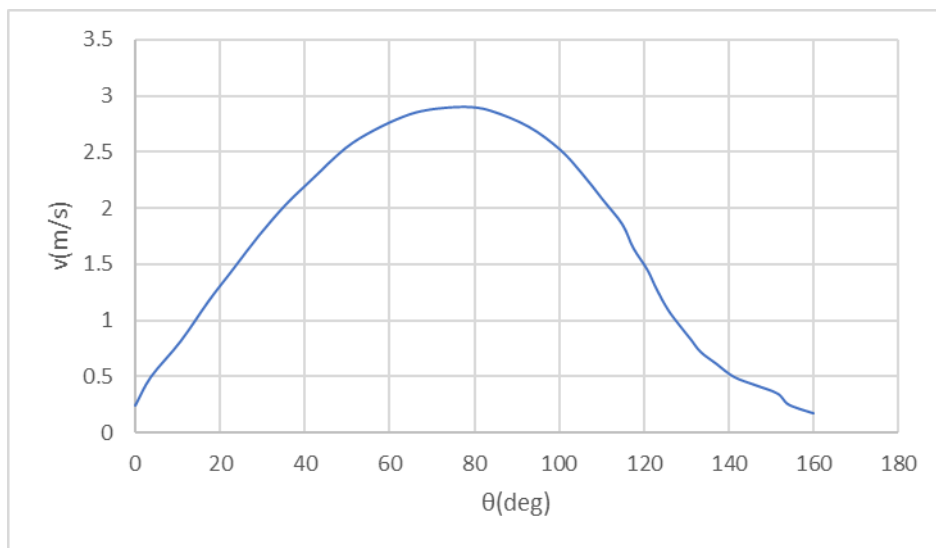


Fig. 21-b Piston velocity in software simulation

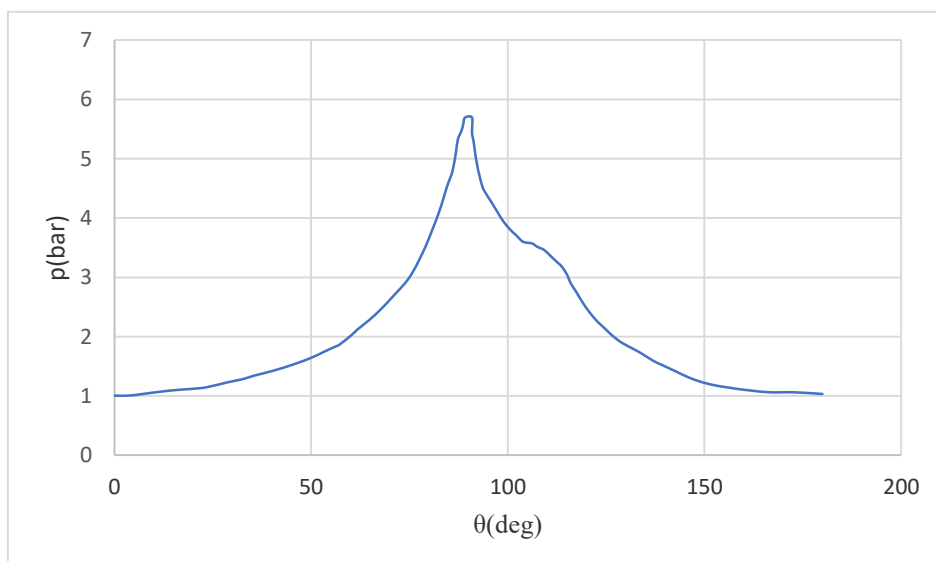


Fig. 21-c cylinder pressure in software simulation

7. Comparison of Extracted Results and Conclusions

A- The results obtained from the analysis of the diagrams of pressure cylinder from software simulation and experimental is showing a large behavioral similarity in the extracted graph (Fig.22).

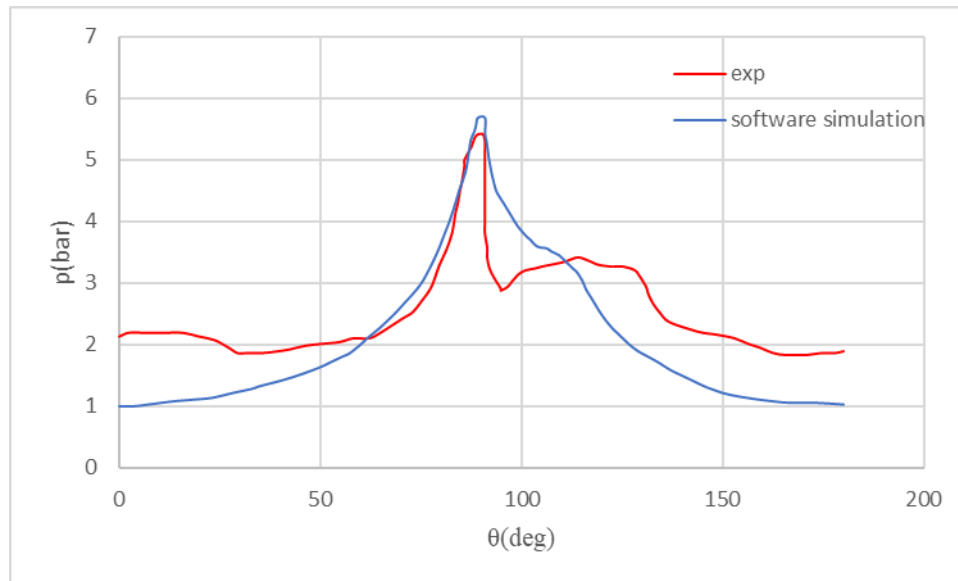


Fig. 22 Rotation angle pressure variations in software simulation and experimental solution

B- The results obtained from the analysis of engine parts in software indicated that the area of thorns installed on the engine shaft was one of the weakest areas and, in case of overloading, it will lead to failure, which in practice was observed that the shaft reinforcement will be one of the most necessary cases (Fig. 23).

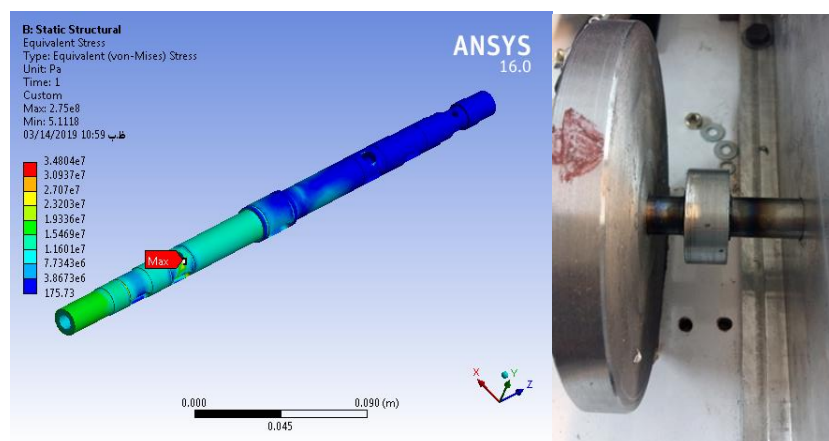


Fig. 23 The weakest shaft area in software and experimental

C- analysis of rotary valve diagrams from software simulation and design predicted diagrams indicate simulation accuracy with acceptable error percentage (Fig 24).

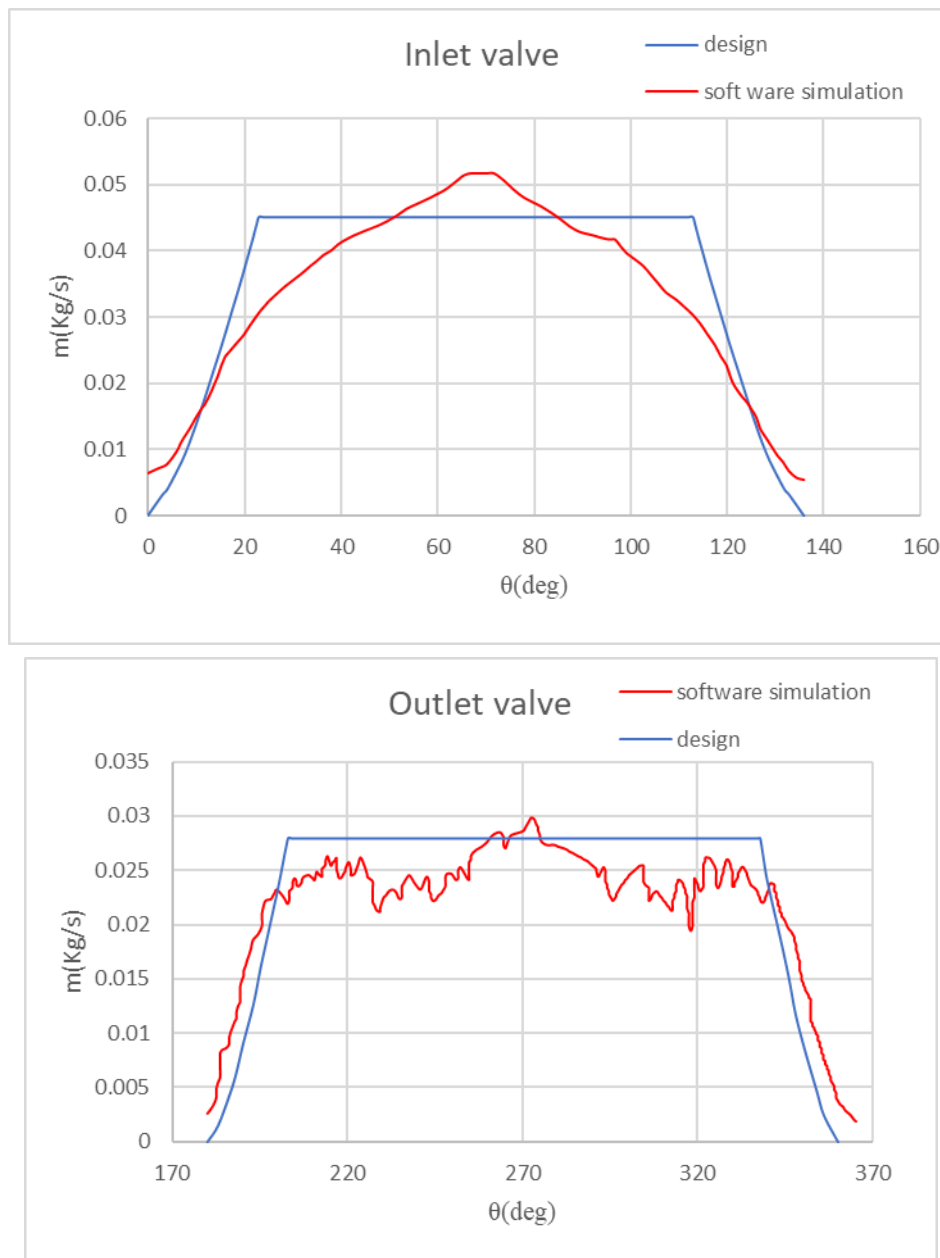


Fig. 24 The rotary valves diagram

D- The exergy available in the pressure range of 2 bar of the gauge to 5 bar will be equal to 27.34 kJ, while the energy obtained in the experimental state was equal to 1.98 kJ. Therefore, the efficiency of the engine according to the ratio of these values equal to 7%..

References

1. Saidur R, Rahi NA, Hasanuzzaman M (2010) A review on compressed-air energy use and energy savings. *Renew Sustain Energy Rev* 14:1135–1153
2. Rouindeja K, Samadanib E, Fräsera RA (2020) A comprehensive data-driven study of electrical power grid and its implications for the design, performance, and operational requirements of adiabatic compressed air energy storage systems. *Appl Energy* 257:1-17
3. Ilamas B, Orteg MF, Barthelemy G, Godos ID, Aciend FG (2020) Development of an efficient and sustainable energy storage system by hybridization of compressed air and biogas technologies. *Energy Convers Manag* 210:112695
4. Chen I, Zheng T, Mel Sh, Xue X, Liu B, Lu Q (2016) Review and prospect of compressed air energy storage system. *J Mod Power Syst* 4:29–541
5. Ibrahima H, Belmokhtara K, Ghandourb M (2015) Investigation of Usage of Compressed Air Energy Storage for Power Generation System Improving - Application in a Microgrid Integrating Wind Energy. *Energy Procedia* 73:305-316
6. Budt M, Wolf D, Span R, Yan J (2016) A review on compressed air energy storage: Basic principles, past milestones and recent developments. *Appl Energy* 170:250–268

7. Yu Q, Shi Y, Cai M, Xu W (2016) Fuzzy logic speed control for the engine of an air powered vehicle. *Adv Mech Eng* 8:1–11
8. Mikalsen R, Roskilly AP (2007) A review of free-piston engine history and applications. *Appl Therm Eng* 27:2339–2352
9. Shaw D, Yu JJ, Chieh C (2013) Design of a Hydraulic Motor System Driven by Compressed Air *Energies* 6:3149-3166
10. Allam S, Zakaria M (2018) Experimental Investigation of Compressed Air engine Performance. *Int J Eng Invent* 7:13-20
11. Ibrahim H, Youne R, Ilinca A, Dimitrova M, Perron J (2010) Study and design of a hybrid wind–diesel-compressed air energy storage system for remote areas. *Appl Energy* 87:1749–1762
12. Miró I, Gasia J, Cabeza IF (2016) Thermal energy storage (TES) for industrial waste heat (IWH) recovery. *Appl Energy* 179:284–301
13. Fertig E, Apt J (2011) Economics of compressed air energy storage to integrate wind power. *Energy Policy* 39:2330–2342
14. Li Y, Miaoa Sh, Luo X, Yin B, Han J, Wang J (2020) Dynamic modelling and techno-economic analysis of adiabatic compressed air energy storage for emergency back-up power in supporting microgrid. *Appl Energy* 261:114448
15. Mahlia TMJ, Saktisahdan TJ, Jannifar A, Hasan MH, Matseelar HSC (2014) A review of available methods and development on energy storage. *Renew Sustain Energy Rev* 33:532–545
16. Mohammadi A, Ahmadi MH, Bidi M, Joda F, Valero A, Uson S (2016) Exergy analysis of a Combined Cooling, Heating and Power system integrated with wind turbine and compressed air energy storage system. *Energy Convers Manag* 131:1-10
17. Dimitriou P, Tsujimura T (2019) A fully renewable and efficient backup power system with a hydrogen-biodiesel-fueled IC engine. *Energy Procedia* 157:1305–1319
18. Basbous T, Younes R, Ilinca A, Perron J (2012) A new hybrid pneumatic combustion engine to improve fuel consumption of wind–Diesel power system for non-interconnected areas. *Appl Energy* 96:459–476
19. Quazi MA, p. Baskar P (2012) Computer simulation of pneumatic engine operation. *Int J Eng Res Technol* 1:1-16
20. Yung Huang C, Kang Hu C, Jie Yu C, Kuo Sung C (2013) Experimental Investigation on the Performance of a Compressed-Air Driven Piston Engine. *Energies* 6:1731-1745
21. Kantharaj B, Garvey S, Pimm A (2015) Thermodynamic analysis of a hybrid energy storage system based on compressed air and liquid air. *Sustain Energy Technol Assess* 11:159-164
22. Pathak S, Swetha K, Sreedhar V, Prabhakar VSV (2014) Compressed air vehicle: a review. *Int J Mech Product Eng* 2014:2320-2092
23. Dimitrova Z, Maréchal F (2015) Gasoline hybrid pneumatic engine for efficient vehicle powertrain hybridization. *Appl Energy* 151:168–177
24. Yu Q, Cai M (2015) Experimental Analysis of a Compressed Air Engine. *J Flow Control Measur Visualiz* 3:144-153
25. Liu CM, You JJ, Sung CK, Huang CY (2015) Modified intake and exhaust system for piston-type compressed air engines. *Energy* 90:516-524
26. Marvania D, Subudhi S (2017) A comprehensive review on compressed air powered engine. *Renew Sustain Energy Rev* 70:1119-1130
27. Liu CM, Huang CL, Sung CK, Huang CY (2016) Performance analysis of a two-stage expansion air engine. *Energy* 115:140-148
28. Liu CM, Wang YW, Sung CK, Huang CY (2017) The Feasibility Study of Regenerative Braking Applications in Air Hybrid Engine, the 8th International Conference on Applied Energy –ICAE2016. *Energy Procedia* 2017:4242- 4247
29. Fang Y, Lu Y, Roskilly AP (2018) Experimental study of a pneumatic engine with heat supply to improve the overall performance. *Appl Therm Eng* 134:78-85
30. Bravo RRS, Negri VJ, Oliveir AAM (2018) Design and analysis of a parallel hydraulic – pneumatic regenerative braking system for heavy-duty hybrid vehicles. *Appl Energy* 225:60–77
31. Singh BR, Singh O (2012) Study of Compressed Air Storage System as Clean Potential Energy for 21st Century. *Global J Res Eng Mech* 12:1-14
32. Norton RL (2004) *Design of machinery*, 3rd ed., McGraw-Hill
33. Mitianiec W (2017) *Modern Pneumatic and Combustion Hybrid Engines, Improvement Trends for Internal Combustion Engines, modern pneumatic and combustion hybrid engines*, Intech Open.
34. Jorge Martins, Carlos Pereira, and F.P. Brito. (2016). A New Rotary Valve for 2-Stroke Engines Enabling Over-Expansion, SAE Technical Paper, 2016-01-1054
35. M. Kordi1, V. Esfahanian. (2016). Axial vane rotary engines preliminary design by quasi dimensional modeling technique, *The Journal of Engine Research*, Vol. 41 (Winter 2016), pp. 41-53